

AD-A191 141

TRANSPARENT GLASS CERAMICS DOPED BY CHROMIUM(III) AND
CHROMIUM(III) AND N. (U) HEBREW UNIV JERUSALEM (ISRAEL)
DEPT OF INORGANIC AND ANALYTIC.. R REISFELD 31 MAR 86

1/1

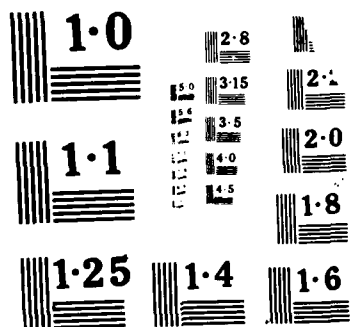
UNCLASSIFIED

DAJA45-85-C-0051

F/G 11/2

NL





AD-A191 141

4697 ms. 01

DTIC FILE COPY

②

TRANSPARENT GLASS CERAMICS DOPED BY CHROMIUM(III)
AND CHROMIUM(III) AND NEODYMIUM(III) AS NEW MATERIALS
FOR LASERS AND LUMINESCENT SOLAR CONCENTRATORS

Research supported by U.S. Army
under Contract No. DAJA 45-85-C-0051

Progress Report
1.10.85 - 31.3.86

Submitted by

Professor Renata Reisfeld
Department of Inorganic and Analytical Chemistry
The Hebrew University of Jerusalem
Jerusalem 91904 Israel

to

European Office of the U.S. Army and
223/231 Old Marylebone Rd.
London WC1 5TH
England

Army Materials and Mechanical
Research Center, Watertown,
Massachusetts 02172
U.S.A.

DTIC
ELECTE
S FEB 17 1988 D
E

This document has been approved
for public release and sale in
distribution is unlimited

88 2 71 086

Summary

In our efforts to develop new materials based on Cr(III) doped transparent glass ceramics we have prepared a variety of glass ceramics with Cr(III) in $\text{SiO}_2\text{-Al}_2\text{S}_3\text{-RO}$ (R = Mg, Ca, Zn).

Spectroscopic properties (absorption and emission) as well as luminescence lifetimes of ^4T and ^2E of Cr(III) were measured.

A correlation was found between the crystalline phases obtained after appropriate heat treatment as determined by X-ray diffraction and the spectroscopic data.

Interpretation was made based on the experimental results as to the position of Cr(III) in various crystalline phases.

The results were summarized in a paper entitled "Transparent glass-ceramics doped by Cr(III): Spectroscopic properties and characterization of crystalline phases" by A. Kiselev, R. Reisfeld, A. Buch and M. Ish-Shalom and submitted to the Journal of Noncrystalline Solids.

In the near future we shall study the experimental conditions of glass-ceramics preparation using interchangeably electric and gas furnaces. In addition to spectroscopic and X-ray measurements of the samples we plan to perform a series of EPR measurements which will enable us to distinguish between various species of Cr(III).

Accession For	
NTIS GRA&I	<input checked="" type="checkbox"/>
DTIC TAB	<input checked="" type="checkbox"/>
Unannounced	<input type="checkbox"/>
Justification	
By	
Distribution/	
Availability Codes	
Dist	Avail and/or Special
A-1	



Note from the author's correspondence

March 31 - April 4, 1986

Vilamoura (Algarve) Portugal

OPTICAL PROPERTIES OF RARE-EARTHS AND TRANSITION METAL IONS IN FLUORIDE GLASSES.

RENATA REISFELD

DEPARTMENT OF INORGANIC AND ANALYTICAL CHEMISTRY
THE HEBREW UNIVERSITY OF JERUSALEM, JERUSALEM 91904, ISRAEL.

1. ABSTRACT

The absorption spectra of chromium(III) and nickel(II) at octahedral sites in a zirconium barium fluoride glass are analyzed and compared with vitreous and crystalline mixed oxides, suggesting slightly longer Cr-F and Ni-F distances than in crystalline fluorides. Laser properties of rare earth ions in fluoride glass (ZBLA) having composition of $57\text{ZrF}_4 \cdot 13.34\text{BaF}_2 \cdot 5\text{LaF}_3 \cdot 7.4\text{AlF}_3$ or (PBLA) having composition of $36\text{PbF}_2 \cdot 24\text{ZnF}_2 \cdot 35\text{GaF}_3 \cdot 3\text{YF}_3 \cdot 2\text{AlF}_3$ for Nd(III) were calculated. Pumping efficiencies, lifetimes of excited and terminal levels and stimulated peak cross-sections are presented. It is shown that multiphonon relaxations (in the case of energy difference less than 3000 cm^{-1}) are always orders of magnitude lower in the fluoride glass than in the tellurite glass and the inhomogeneous width is consistently smaller in fluoride glass than in tellurite glass, which was chosen as a model for oxide glass. No significant difference was found for concentration quenching between the two kinds of glasses. Energy transfer between Mn(II) and Nd(III) can increase pumping efficiencies of Nd(III) lasers (Kashner, ISRAEL).

2. INTRODUCTION

Fluoride glasses containing about 50 mole% of ZrF_4 which can be replaced by HfF_4 or ThF_4 [1-3], colloquially called ZBLA glass, have been considered as materials for fiber optics in the range of $0.3\text{-}5\text{ }\mu\text{m}$ [4]. Another important category of fluoride glasses containing zinc(II) (or manganese), gallium (III) and lead(II) fluorides was invented [5,6] at the University of Maine, Le Mans (PBLA glass). The absorption spectra and luminescence of $4f^{11}$ erbium(III) and $3d^5$ manganese (II), and the mutual energy transfer between excited states of these two species were studied in such a glass [7]. In ZBLA glass, the luminescence of $4f^2$ praseodymium(III) [8,9], $4f^6$ europium(III) [10,42], $4f^{10}$ holmium(III) [11,12] and erbium(III) [13-15] occurs from more excited J-levels than usual, the lower limit still allowing perceptible luminescence for the energy gap between the emitting J-level and the closest lower-lying J-level being 2000 cm^{-1} (0.25 eV), some 2 to 4 times smaller than in nearly all other glasses and crystals. It may be noted that this rich emission spectrum to several J-levels besides the groundstate is observed also at room temperature.

The superior optical characteristics of fluoride glasses for IR fiber optic applications also provide an ideal medium or host enabling the glass to be integrated into a system acting as a laser light source as well as the actual waveguide material. The spectroscopic and fluorescent properties of Nd(III) containing fluorozirconate glasses have been reported by Weber in work with the Lucas-Poulain group at Rennes [16] and optical absorption of 3d transition metal ions such as Fe, Co, Ni and Cu by Ohishi et al. [17].

page 1

luminescence and nonradiative relaxation of rare earths in amorphous oxide materials has recently been reviewed [18].

3. CHROMIUM(III) AND NICKEL(II) IN ZBLA GLASSES

The absorption spectra of Cr(III) and Ni(II) at room temperature are shown in Fig 1. The observed band peaks, and ligand field and Racah parameters are presented in Table I.

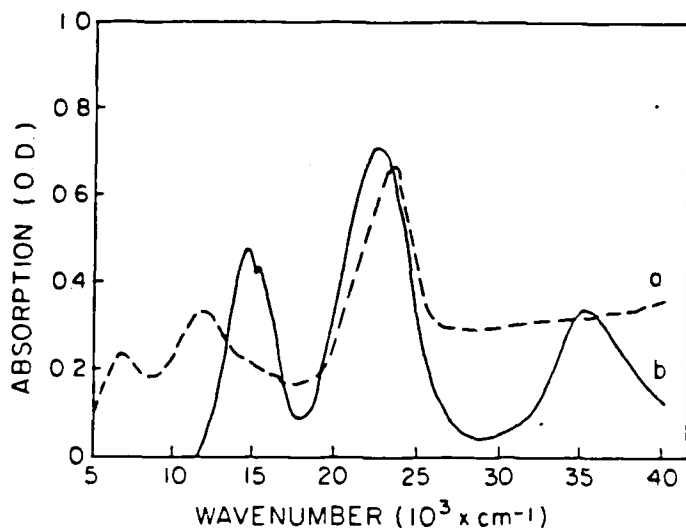


FIGURE 1. Absorption spectra of a) Cr(III) and b) Ni(II) in ZBLA ($56.75\text{ZrF}_4 \cdot 34.25\text{BaF}_2 \cdot 4.5\text{LaF}_3 \cdot 4\text{AlF}_3 \cdot 0.5(\text{NiF}_2, \text{CrF}_3)$) at room temperature.

From the absorption spectra of Cr(III) and Ni(II) in ZBLA glass, both in the work of Reisfeld et al. [19] and in that of Ohishi et al. [17], as well as from the absorption spectra of these ions in PBLA glass [5], it can be demonstrated that the site symmetry for both Cr(III) and Ni(II) in these glasses is close to cubic octahedral symmetry. Sites of lower symmetry would have relatively much stronger absorption bands. Such a situation could be predicted for PBLA glass in view of the feasible substitution of Zn(II) and Ga(III) by Cr(III) of comparable radius.

Also it is shown that almost all Cr(III) and a large majority of all paramagnetic Ni(II) complexes in solution as well as solid compounds show the coordination number $N = 6$ with octahedral symmetry. However it is not perfectly trivial that Cr(III) and Ni(II) in ZBLA glass (known from Raman spectra [20] to have more complicated coordination behaviour) turns out to be octahedral to a high approximation. The sub-shell energy difference dq (also designated as Δ) corresponds to the maximum (or strictly to the center of gravity) of the first spin-allowed transition. The Racah parameter [21,22] of interelectronic repulsion B is derived from the diagonal sum rule. Also it is known that:

$$B = (\sigma_2 + \sigma_3 - 3\sigma_1) / 15 \quad (1)$$

Such a derivation is rarely possible in Cr(III) because the third spin-allowed transition is usually hidden by electron transfer bands or other intense absorption. In such Cr(III) cases, B can be derived [23] from σ_1 and σ_2 alone, providing $B = 850 \text{ cm}^{-1}$ for Cr(III) in ZBLA and PBLA. The nephelauxetic ratio, β , is the ratio between B from Eq.(1) and B_0 for the gaseous ion, 918 cm^{-1} for Cr^{3+} and 1041 cm^{-1} for Ni^{2+} . It is interesting to compare the parameters of Table I with related materials (vitreous and crystalline oxides) which were compiled for 36 Cr(III) cases [24].

The value for dq of Cr(III) in ZBLA glass is distinctly lower than 16100 cm^{-1} reported [25] for the cubic elpasolites $\text{K}_2\text{NaGa}_{0.95}\text{CrO}_{0.05}\text{F}_6$ and K_2NaCrF_6 suggesting 1.5 percent (0.03 Å) longer average Cr-F distances in the glass than in the crystal, as discussed below for analogous Ni(II) cases. The parameters in Table I are closer to CrF_6^{3-} in solution [21] having $dq=15200 \text{ cm}^{-1}$ and $B=820 \text{ cm}^{-1}$ according to Claus Shaffer. They fall inside the intervals $dq=14500$ to 16400 cm^{-1} and $B=620$ to 850 cm^{-1} given [26] for Cr(III) in 14 highly different mixed oxide glasses, and may also be compared with $dq=17450$ and $B=725 \text{ cm}^{-1}$ for $\text{Cr}(\text{OH})_6^{3+}$. The first absorption band of the fluorides and many oxide cases, shows a complicated structure because the first two doublet levels 2E and 2T_1 almost coincide with 4T_2 providing additional complications of spin-orbit coupling. The most prominent narrow peak occurs at 654 nm (15300 cm^{-1}) in our ZBLA glass, to be compared with 15430 cm^{-1} in a zirconium barium thorium fluoride glass [26], which should represent the position of 2E to a good approximation.

Since 4T_2 stretches distinctly well below 2E one expects any luminescence to be a broad-band transition between the two lowest quartet levels. Only very weak fluorescence of Cr(III) was seen in fluorophosphate glass [26] and in ZBLA [19]. Lifetimes as well as the peak emissions of Cr(III) in ZBLA glass are presented in Table II. The short lifetimes form a striking contrast, not only to the cubic elpasolites [25] with temperature-dependent lifetimes in the range 0.2 to 0.6 msec, but also to Cr(III) in a lithium lanthanum phosphate glass [27] with lifetimes around 0.02 msec (0.025 msec at the same low Cr(III) concentration as in the ZBLA glass) and a quantum yield up to 0.23. Much higher quantum yields are observed in glass-ceramics containing crystallites (much smaller than 400 nm) of spinel-type $\text{MgAl}_2\text{CrO}_4$ and the isotypic gahnite $\text{ZnAl}_2\text{CrO}_4$ [28] and other types [24,29,30]. Such glass-ceramics may be useful as laser materials, conceivably replacing the crystalline alexandrite $\text{Al}_2\text{CrBeO}_4$.

The dq value for nickel(II) in ZBLA glass is unusually small when compared with 8800 NiO; 8650 NiMg_{1-x}O; 8500 Ni(OH)₂; 7400 NiTiO₃; and 7300 NiMg_{1-x}TiO₃ (all values [21] in cm^{-1}). It is particularly interesting to compare with crystalline fluorides [21,31] such as 7800 spinel-type Li_2NiF_4 ; 7700 rutile-type NiF_2 ; 7500 perovskite-type KNiF_3 ($B=950$ and 960 cm^{-1} in the two latter compounds to be compared with 940 cm^{-1} in $\text{Ni}(\text{OH})_2$ and 840 cm^{-1} in $\text{NiMg}_{1-x}\text{TiO}_3$). Rüdorff, Kändler and Babel [31] pointed out that such variations can be ascribed to slightly varying internuclear distances R. In this perspective ZBLA seems to have Ni-F distances on the average 1.6% (0.03 Å) longer than crystalline KNiF_3 . In mixed oxides more dramatic effects can occur, dq of Ni(II) being decreased to 6000 cm^{-1} in ilmenite-type $\text{NiCd}_{1-x}\text{TiO}_3$ (isotypic with NiTiO_3 and MgTiO_3) and, as shown by Reinen, to only 4800 cm^{-1} in the perovskite (elpasolite superstructure?) $\text{Ba}_2\text{Ca}_{1-x}\text{TeNiO}_6$ [21]. However in such substituted crystals (like in the classical case of ruby CrAl_2O_3) a weak doubt always remains whether the distance M-X between M carrying a partly filled shell and the closest neighbour atoms X fully adapts to the internuclear distances in the closed-shell host lattice. More convincing evidence comes from the

static high pressure (especially for atoms [32] on special positions) and substituted crystals remain the only technique of significantly increasing R. A direct determination of R (with a precision of about 0.02Å) is accessible to EXAFS using the X-ray absorption edge of the substituting M even in low concentration [33].

TABLE I: Optical transitions of Cr(III) and Ni(III) in fluoride glasses

ION	TRANSITION ASSIGNMENT	BAND POSITION		PARAMETERS	
		OBSERVED [cm ⁻¹]		[cm ⁻¹]	
		[17]	[19]	[17]	[19]
Cr(III)	$4A_{2g}(^4F) \rightarrow 4T_{2g}(^4F)$	14749	14800		
*	$4A_{2g}(^4F) \rightarrow 2E_g(^2G)$	15385	-	Dq=1475	Dq=1480
*	$4A_{2g}(^4F) \rightarrow 4F_{1g}(^4F)$	22472	22500	B=847	B=850
*	$4A_{2g}(^4F) \rightarrow 4T_{1g}(^4P)$	34483	34700	C=3136	
Ni(II)	$3A_{2g}(^3F) \rightarrow 3T_{2g}(^3F)$	6536	6900		
*	$3A_{2g}(^3F) \rightarrow 3T_{1g}(^3F)$	11364	11500	Dq=663	Dq=690
*	$3A_{2g}(^3F) \rightarrow 3E_g(^1D)$	14925	-	B=956	B=970
*	$3A_{2g}(^3F) \rightarrow 3T_{1g}(^3P)$	22936	23300	C=4006	

Nephelauxetic parameter β in ZBLA glass [19] is 0.926 for Cr(III) and 0.932 for Ni(II)

TABLE II: Lifetimes of Nd(III) (876 nm emission) and Cr(III) (~800nm emission) in ZBLA glass.

DOPANT 1	DOPANT 2	EXCITATION λ , [nm]	EMISSION λ , [nm]	DECAY, [μsec]		
				τ_1	τ_2	τ_3
-	0.5 Cr	465	797	1.4	3.0	6.0
0.5 Mn	0.5 Cr	414	790	0.4	1.0	3.1
0.5 Nd	0.5 Cr	337	804	0.6	1.2	3.1
0.5 Mn	0.5 Cr	337	804	0.5	1.9	3.9
0.5 Nd	0.5 Cr	450	876	381	410	410
0.5 Nd	0.5 Cr	579	876	380	405	-

The only possibility of luminescence of Ni(II) in ZBLA glass would be at the foot (some 6000 cm⁻¹) of the first absorption band, but we did not detect any. The spin-forbidden absorption band due to the first singlet level ¹E corresponds to the rather broad shoulder at 15000 cm⁻¹ (see Fig.1)

comparable to the peak [31] of crystalline Ni(II) fluorides between 15000 and 15400 cm^{-1} .

4. NEODYMIUM(III) IN FLUORIDE GLASSES:

4.1. Intensity parameters and radiative transitions of Nd(III)

The absorption spectrum of Neodymium(III) serves as a basis for a complete set of predictions of transition rates within the $4f^3$ configuration of Nd(III). The procedure is based on the theory of Judd - Ofelt and is described in detail elsewhere [14]. Here we describe briefly the main steps of its evaluation;

According to the theory the otherwise forbidden transitions within the f-f configuration of rare-earths become slightly allowed by admixing of wavefunctions of the f-f configuration with odd components of crystal field potential. The intraconfigurational transitions then become subject to a new set of selection rules and oscillator strengths of the transitions depend parametrically on the three phenomenological parameters Q_2, Q_4, Q_6 . Reduced matrix elements for the transitions are almost invariant in respect to the crystal field strength [34] and were tabulated for all rare earths ions [35].

The optical transitions of rare earths in solids are predominantly of electric dipole character and their spectral intensities can be described using the treatment of Judd and Ofelt. In this approach the line strength S of a transition between two J states is given by the sum of products of empirical intensity parameters Q_t and matrix elements of tensor operators $U^{(t)}$ of the form

$$S(J, J') = e^2 \sum_t Q_t |\langle aJ || U^{(t)} || bJ' \rangle|^2 \quad (2)$$

where $t=2,4,6$

The values of Q_t are obtained from a least-squares fit of measured and calculated absorption line strengths and typically have an experimental uncertainty of about 10%. The integrated intensities of the absorption bands yield Q_t 's which are an effective average over the different rare earths environments in the glass.

The most significant factor determining the values is the strengths of the odd-order terms in the expansion of the local field at the rare earth sites. These in turn are affected by the nearest-neighbour anion(s) and cations. For a given glass former systematic changes of Q_t have been observed with the changes in the size and charge of network modifier ions [36].

The three omega's are determined by solving an overdetermined set of linear equations built by equating the measured oscillator strengths with the sum of products of the unknown omega's with the appropriate reduced matrix elements. The three omega's found from the solution are put into a computer program which calculates all the radiative transition rates possible in the system analyzed. The omega parameters for ZBLA and PBLA glasses are given in Table III. The oscillator strengths of Nd(III) are given in Table IV. Generally Q_2 is lower in fluoride than in oxide glasses, which is of no consequence for the $F_{3/2} - I_{11/2}$ laser transition for which $U^{(2)} = 0$.

Table III: Omega parameters in ZBLA and PBLA glasses.

GLASS	REFERENCE	Ω_2 .[pm^2]	Ω_4 .[pm^2]	Ω_6 .[pm^2]
PBLA	[19]	1.01 ± 0.28	3.73 ± 0.35	6.19 ± 0.43
ZBLA	[19]	1.10 ± 0.25	3.80 ± 0.30	5.53 ± 0.20
ZBLA	[16]	1.95 ± 0.26	3.65 ± 0.38	4.17 ± 0.17

4.2 Fluorescent lifetimes and nonradiative transitions

The calculation of nonradiative transfer rates due to multiphonon decay is accomplished by subtracting the calculated radiative rates from the reciprocals of the integrated lifetimes of as many as possible energy levels of the rare earth ions and plotting the logarithms of the numbers against energy gaps between the levels and their nearest lower neighbour. Then the two parameters of the exponential multiphonon decay rate law are calculated; the exponential parameter α from the slope of the plot and the electronic factor B from its intercept [37].

Since only three energy levels of Nd(III) in fluoride glasses have lifetimes long enough to be measurable the α and B were determined from 3 points only. Fortunately the result, which is $\alpha = 0.0053 \pm 0.0005$ and $B = 1.63 \pm 0.1 \times 10^{10}$, agrees well with other sets of data which were measured on Ho(III) in ZBLA glass in our laboratory [8]. The parameters are substituted into formula (3)

$$W_{nr} = B \exp[-\alpha \Delta E] \quad (3)$$

where ΔE is the energy gap from the electronic level to its next lower neighbour. The entire set of transition rates is calculated, now with the nonradiative transition rates included [37].

The result of such a procedure is shown in Table IV for Nd(III) in PBLA glass. The calculated oscillator strengths agree well with the measured values. The omega's calculated from our ZBLA glass compare well with the values obtained by Lucas et al.[16] in their study of Nd(III) in ZBLA glass. The last two columns in Table IV compare calculated lifetimes with the measured lifetimes. The outstanding property of fluoride glasses is the relatively long-lived luminescence from levels which are separated only by a small energy gap to the next lower level [12]. Here we are able to record and measure the lifetimes of emissions from two levels; thermalized $D_{3/2}$ (361nm) and $P_{3/2}$ (387nm). The first three emission lines are identified as belonging to the following transitions: $D_{3/2} - I_{9/2}$ (361nm), $D_{3/2} - I_{11/2}$ (381nm) and $D_{3/2} - I_{13/2}$ (412nm). The next, much weaker group of lines belong mainly to the transitions from $P_{3/2}$. The spectroscopic assignments of these lines are given in Table IV for Nd(III) in PBLA glass alone and in Table V for Nd(III) with Mn(II). The integrated lifetimes of these emissions are not influenced by the presence of Mn(II) ions. In both Tables the first group of transitions having integrated lifetimes varying from 1.4 to 2.1 μsec belongs to the transitions from the D manifold. Its predicted lifetime is 0.97 μsec . The second group of lifetimes (15-20 μsec) belongs to the transitions from $P_{3/2}$. Its predicted lifetime is 13.6 μsec . The predictions which are based on the theory of Judd-Ofelt combined with the exponential multiphonon law are not expected to give better agreement [8].

Table IV: Oscillator strengths and lifetimes of Nd(III) in PBLA glass:
(36PbF₂, 24ZnF₂, 35GaF₃, 2AlF₃, 3YF₃, 2LaF₃, 2NdF₃)

TRANSITION	WAVELENGTH [nm]	OSCILLATOR STRENGTHS		LIFETIMES, [μsec]	
		OBSERVED	CALCULATED	OBSERVED	CALCULATED
$^4D_{1/2} - ^4I_{9/2}$	354	9.04	4.27	-	0.00007
$^4D_{5/2} - ^4I_{9/2}$	357	9.04	1.27	-	0.00009
$^4D_{3/2} - ^4I_{9/2}$	361	-	3.7	1.5	1.0
$^4D_{3/2} - ^4I_{11/2}$	381	-	11.5	1.4	1.0
$^4D_{3/2} - ^4I_{13/2}$	412	-	1.15	1.2	1.0
$^4D_{3/2} - ^4F_{5/2}$	637	-	5.10	1.70	1.0
$^2P_{3/2} - ^4I_{9/2}$	387	0.09	0.05	-	13.6
$^2P_{3/2} - ^4I_{11/2}$	419	-	1.00	19.0	13.6
$^2P_{3/2} - ^4I_{13/2}$	454	0.04	0.04	15.0	13.6
$^2P_{3/2} - ^4I_{15/2}$	502	-	0.01	18.0	13.6
$^2P_{3/2} - ^4H_{9/2}$	746	-	2.40	18.0	13.6
$^2P_{3/2} - ^4F_{9/2}$	886	-	2.40	18.5	13.6
$^2D_{5/2} - ^4I_{9/2}$	426-440	0.17	0.04	-	0.0008
$^2P_{1/2} - ^4I_{9/2}$		0.17	0.09	-	0.3000
$^4G_{11/2} - ^4I_{9/2}$	475	1.38	0.21	-	0.00003
$^2D_{3/2} - ^4I_{9/2}$	478	1.38	0.35	-	0.00005
$^2G_{9/2} - ^4I_{9/2}$	483	1.38	0.42	-	0.1000
$^4G_{9/2} - ^4I_{9/2}$	510	1.38	1.50	-	0.0002
$^4G_{7/2} - ^4I_{9/2}$	523	6.98	2.70	-	0.2500
$^2G_{7/2} - ^4I_{9/2}$	577	9.78	2.74	-	0.00015
$^4G_{5/2} - ^4I_{9/2}$	577	9.78	7.30	-	0.0040
$^2H_{11/2} - ^4I_{9/2}$	620	0.18	0.18	-	0.0200
$^4F_{9/2} - ^4I_{9/2}$	678	0.37	0.66	-	0.0100
$^4F_{7/2} - ^4I_{9/2}$	732	6.41	5.70	-	0.00004
$^4S_{3/2} - ^4I_{9/2}$	743	6.41	0.03	-	0.0009
$^2H_{9/2} - ^4I_{9/2}$	797	7.13	1.40	-	0.00006
$^4F_{5/2} - ^4I_{9/2}$	802	7.13	6.20	-	0.0090
$^4F_{3/2} - ^4I_{9/2}$	860	1.92	2.20	190.0	337.00

The integrated lifetime of $^4F_{3/2}$ level of Nd(III) is 190 μsec in $36\text{PbF}_2 \cdot 24\text{ZnF}_2 \cdot 35\text{GaF}_3 \cdot 2\text{AlF}_3 \cdot 3\text{YF}_3 \cdot 2\text{LaF}_3 \cdot 2\text{NdF}_3$, 330 μsec in $36\text{PbF}_2 \cdot 24\text{MnF}_2 \cdot 35\text{GaF}_3 \cdot 2\text{AlF}_3 \cdot 3 \cdot 8\text{LaF}_3 \cdot 0.2\text{NdF}_3$ and about 400 μsec in $56.50\text{ZrF}_4 \cdot 34.00\text{BaF}_2 \cdot 4.5\text{LaF}_3 \cdot 4\text{AlF}_3 \cdot 0.5\text{CrF}_3 \cdot 0.5\text{NdF}_3$ (Table II). Here the prediction which is 450 μsec for ZBLA and 337 μsec for PBLA is near to the experimental result, while the short 190 μsec is due to the cross-relaxation mechanism, vide infra. A summary of lifetimes of Nd(III) ions in various samples is shown in Tables II, IV and V.

TABLE V. Neodymium in PBLA glass: $35\text{PbF}_2 \cdot 24\text{MnF}_2 \cdot 35\text{GaF}_3 \cdot \text{AlF}_3 \cdot (4-x)\text{LaF}_3 \cdot x\text{NdF}_3$

TRANSITION	X	WAVELENGTH, [nm]		LIFETIMES, [μsec]				RISETIME	
		EXCITATION	EMISSION	τ_1	τ_2	τ_3	τ_{in}	SHORT	LONG
$^4D_{3/2} - ^4I_{9/2}$	0.2	337	360	1.4	1.5	1.8	1.5	<0.5	-
$^4D_{3/2} - ^4I_{11/2}$	0.2	337	381	1.8	2.0	2.3	2.0	<0.5	-
?	0.2	337	810	471	-	-	471	0.60	44
?	0.2	407	810	614	-	-	614	0.60	49
$^4F_{3/2} - ^4I_{9/2}$	0.2	337	865	567	507	499	500	1.5	70
$^4F_{3/2} - ^4I_{9/2}$	0.2	407	865	632	642	-	637	1.5	85
$^4F_{3/2} - ^4I_{9/2}$	0.2	579	865	265	327	345	330	-	7.0
$^4D_{3/2} - ^4I_{9/2}$	0.2	337	361	1.3	1.5	1.7	1.5	<0.5	-
$^4D_{3/2} - ^4I_{11/2}$	0.2	337	381	1.2	1.4	1.8	1.5	<0.5	-
$^2P_{3/2} - ^4I_{11/2}$	2.0	337	419	18.0	20.0	21.0	20.0	<0.5	1.5
$^2P_{3/2} - ^4I_{15/2}$	2.0	337	499	19.0	18.0	18.0	18.0	<0.5	1.5
$^4D_{3/2} - ^4F_{5/2}$	2.0	337	637	1.8	-	-	1.8	<0.5	-
$^2P_{3/2} - ^2H_{9/2}$	2.0	337	743	18.0	18.0	20.0	18.0	<0.5	1.5
$^4F_{3/2} - ^4I_{9/2}$	2.0	337	867	176	215	238	220	-	3.0
$^4F_{3/2} - ^4I_{9/2}$	2.0	407	867	180	210	240	220	-	3.0
$^4F_{3/2} - ^4I_{9/2}$	2.0	579	867	172	192	210	196	-	3.0
$^2P_{3/2} - ^4F_{9/2}$	2.0	337	886	18.0	24.0	28.0	25.0	<0.5	2.5

4.3. Cross-relaxation

Special cases of energy transfer are cross-relaxations when the original system loses the energy ($E_3 - E_2$) by obtaining the lower state E_2 (which may also be the groundstate E_1) and another system acquires the energy by going to a higher state E_2 [37]. Cross-relaxation may take place between the same lanthanide (being a major mechanism for quenching at higher concentration in a given material) or between two differing elements, which happen to have two pairs of energy levels separated by the same amount. The cross-relaxation between a pair of rare earth ions is graphically presented in Fig.3 of [37].

The measured lifetime of luminescence is related to the total relaxation rate by

$$1/\tau = \Sigma W_{nr} + \Sigma A + P_{cr} = 1/\tau_0 + P_{cr} \quad (4)$$

where ΣA is the total radiative rate, ΣW_{nr} is the nonradiative rate and P_{cr} is the rate of cross-relaxation between adjacent ions, and τ_0 is intrinsic lifetime.

The critical radius R_0 for cross-relaxation is defined by

$$P_{cr}(R_0) \cdot (1/\tau_0) = 1 \quad (5)$$

R_0 being the critical distance at which the probability for cross-relaxation P_{cr} equals the sum of radiative and multiphonon relaxations.

The cross-relaxation channel for Nd(III) is $(^4F_{3/2}) + (^4I_{9/2}) \rightarrow 2(^4I_{15/2})$. The critical radii in various glasses are presented in Table VI.

TABLE VI. Critical radii for cross-relaxation of Nd(III) in tellurite and fluoride glasses

COMPOUND	CONCENTRATION [$10^{20}/\text{cm}^3$]	CRITICAL RADIUS[A]	$\tau_{\text{intrinsic}}$ [μsec]	τ_{measured} [μsec]	EXCITATION λ , [nm]
0.5/ZnTe	1.10	4.74 \pm .11	187	178	579
1.6/ZnTe	3.50	5.07 \pm .36	187	130	579
2.7/ZnTe	5.80	5.81 \pm .25	187	102	579
0.5/ZBLA	.85	3.72 \pm .80	455	443	576
2.0/PBLA	1.70	5.07 \pm .61	345	264	576

ZnTe- 35ZnO, 65TeO₂

4.4 Laser action :

The formula for peak cross-section is [38]

$$\sigma = \frac{\lambda^4 A}{8\pi c n^2 \Delta \lambda} [\text{cm}^2] \quad (6)$$

where λ - emission wavelength [cm]

$\Delta \lambda$ - full width at half height of emission band [cm]

n - refractive index

A - radiative transfer probability [sec^{-1}]

Threshold power for transverse pumping is

$$P_{th} = \frac{hc(L_o + L_{res}) \cdot 10^{-7}}{2\lambda \tau_f l F \sigma_p} \quad (7)$$

where L_{res} - resonant power loss due to self-absorption at the laser wavelength which is defined as

$$L_{res} = 2l\alpha N \beta_y / Z$$

(8)

where N - number density of lasing lines

β_y - Boltzmann factor for the terminal laser level

Z - partition function

l - length of laser

Nd(III) the terminal level, $^4I_{11/2}$ for the 1060nm luminescence is positioned at $\sim 2000 \text{ cm}^{-1}$, then $E/kT \sim 10$ at room temperature and the Boltzmann factor is $\sim 4.5 \times 10^{-5}$. For a 1 cm long minilaser at representative values of N and σ :

$L_{res} = 0.2-0.1 \%$.

L_o - Nonresonant loss which is mainly due to the absorption of the medium and loss at mirrors. It is usually taken to be 0 - 1.5%

λ_p - pumping wavelength. In our case it is 806nm of LED, having 25nm bandwidth.

τ_f - lifetime of lasing level.

F_f - Boltzmann population function of the lasing level. The $^4F_{3/2}$ of Nd(III) is split into 2 main bands in glasses. The fraction of the population at the lasing level (R_1) is 0.64 - 0.72R

α_p - absorption coefficient of the pumped level which in our case is centered at 800nm ($^4F_{5/2} + ^2H_{9/2}$) and is obtained by dividing the optical density of the sample by its thickness

Table VII presents the comparison of peak cross-section and threshold pump for laser action of Nd(III) in fluoride, oxide and chalcogenide glasses for transverse pumping. From the Table it can be seen that the laser characteristics for Nd(III) in fluoride glasses are quite similar and even better than in ED-2 glass.

TABLE VII: Spectroscopic and Laser Properties of Nd(III) in Fluoride Glasses as Compared to Chalcogenide and Oxide Glasses

		Laser	Conc.	Abs. coef.	λ	σ [cm ²]	P_{th} [W/cm ²]		τ_f	
Host	Assignment	wavelen.	[cm ³]	at 806nm			$L_o=1\%$	$L_o=1\%$		Ref.
		[nm]	$\times 10^{20}$	[cm ⁻¹]	[nm]	$\times 10^{-20}$	$L_r=0.2\%$	$L_r=0\%$	[usec]	
ZBLA	${}^4F_{3/2} - {}^4I_{11/2}$	1049	2.72	3.14	26.7	2.9	57	-	400	16
PBLA	${}^4F_{3/2} - {}^4I_{11/2}$	1039	4.02	3.57	33.0	2.75	112	-	190	19
PBLA	${}^4F_{3/2} - {}^4I_{13/2}$	1306	4.02	3.57	65.0	0.85	-	256	190	19
ED-2	${}^4F_{3/2} - {}^4I_{11/2}$	1060	1.83	1.27	27.8	2.9	173	-	300	38
ED-2	${}^4F_{3/2} - {}^4I_{13/2}$	1340	1.83	3.14	64.4	0.72	-	590	300	38
ZnTe	${}^4F_{3/2} - {}^4I_{11/2}$	1060	3.46	4.73	29.0	3.6	93	-	130	19
ZnTe	${}^4F_{3/2} - {}^4I_{13/2}$	1340	3.46	4.73	73.0	0.76	-	367	130	19
GLS	${}^4F_{3/2} - {}^4I_{11/2}$	1077	2.63	14.50	-	7.95	11.3	-	100	41
GLS	${}^4F_{3/2} - {}^4I_{13/2}$	1370	2.63	14.50	-	3.60	-	27.7	100	41

ZBLA - 57.0ZrF₄.34.0BaF₂.3.0LaF₃.4.0AlF₃.2.0NdF₃ mole%

PBLA - 36PbF₂.24ZnF₂.35GaF₃.2AlF₃.3VF₃.2LaF₃.2NdF₃ mole%

ED-2 - 60SiO₂.27.5Li₂O.10CaO.2.5Al₂O₃.0.16CeO₂ mole%.2.012Nd₂O₃ wt%

Chalcogenide, GLS - 3Ga₂S₃.0.85La₂S₃.0.15Nd₂S₃

Zinc Tellurite, ZnTe - 35ZnO.65TeO₂ mole%.2 Nd₂O₃ wt%

5. ENERGY TRANSFER FROM MANGANESE(II) TO ERBIUM(III) AND NEODYMIUM(III)

5.1. Energy transfer from Mn(II) to Er(III)

Energy transfer between Mn(II) and Er(III) in PBLA glass having composition $36\text{PbF}_2 \cdot 24(\text{Mn}, \text{Zn})\text{F}_2 \cdot 35\text{GaF}_3 \cdot 5\text{Al}(\text{PO}_3)_3$ doped with Er(III) has been studied recently [7]. The emission of Mn(II) in absence of Er(III) consists of a broad band centered around 630nm and an integrated lifetime of 1.4msec. In the presence of Er(III) the intensity and lifetimes are decreased as a result of energy transfer to the $^4\text{F}_{9/2}$ level of Er(III). The fluorescence of Er(III) arising from $^4\text{S}_{3/2}$ at 543nm has an integrated lifetime of 60μsec in the absence of Mn(II) and is decreased to 10μsec in the presence of Mn(II) as a result of energy transfer to Mn(II). The 666nm luminescence of Er(III) is enhanced in the presence of Mn(II) and has a non-exponential time dependence. The longer component corresponds to the transfer of energy from Mn(II) to Er(III) while the short-lived component is probably due to the cascading down Er(III)-Mn(II)-Er(III) through states above the Stokes threshold of Mn(II).

5.2. Energy transfer from Mn(II) to Nd(III)

The evidence of energy transfer between Mn(II) and Nd(III) in PBLA and ZBLA glass is seen in Figs. 3 and 4 where Nd(III) can be excited via Mn(II) at 337 nm or at 400 nm [43]. The risetime of about 0.1 msec in Figs. 3 and 4 is characteristic of the time at which the energy transfer takes place.

Fig.4 shows the approximately exponential decay with lifetime 0.34 msec by excitation in the Nd(III) band at 579nm, the emission being measured at

876nm. When the excitation is done at 404nm, at the low-energy edge of the narrow $^6\text{S} - ^4\text{G}$ absorption band of Mn(II), the same Nd(III) emission at 876nm shows a rise-time of about 0.1 msec followed by an exponential decay with the lifetime 1.45 msec. Such storage of energy in the lowest quartet of Mn(II) was previously observed [7] for Mn(II) and Er(III) in zinc gallium lead fluoride glass. The energy scheme for transfer between Mn(II) and Nd(III) in such a glass is presented in Fig.2. In the absence of Nd(III) the luminescence of Mn(II) in ZBLA measured at 545nm shows an approximately exponential decay curve with lifetime between 13 and 14 msec (note the concentration of Mn(II) of 1 wt%). This mechanism of energy storage has obvious potential applications in laser materials

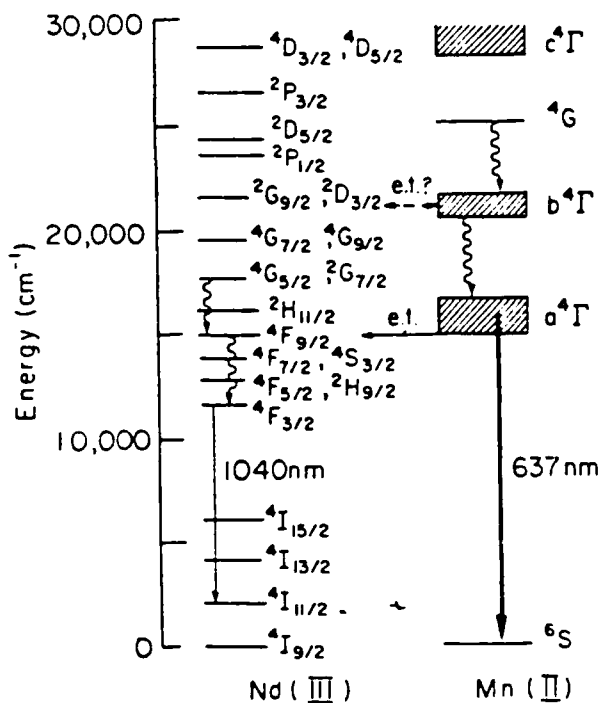


Fig.2 Scheme of energy levels of Nd(III) and Mn(II) in fluoride glass.

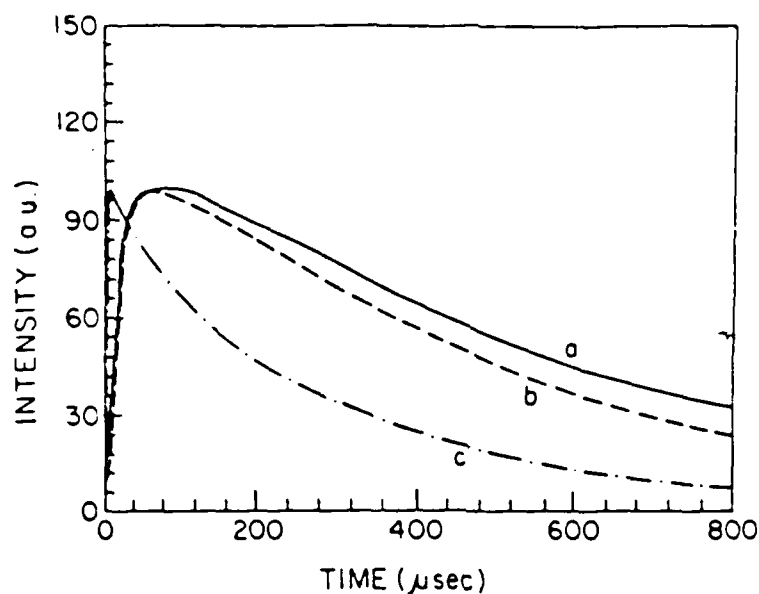


Fig.3 Luminescence decay curves of Nd(III) in PBLA glass ($36\text{PbF}_2, 24\text{MnF}_2, 35\text{GaF}_3, 2\text{AlF}_3, 3.8\text{LaF}_3, 0.2\text{NdF}_3$). a) Excitation 407nm. Lifetime 637 μsec . Risetime 85 μsec . b) Excitation 337nm. Lifetime 500 μsec . Risetime 70 μsec . c) Excitation 579nm. Lifetime 330 μsec . Risetime 2.0 μsec .

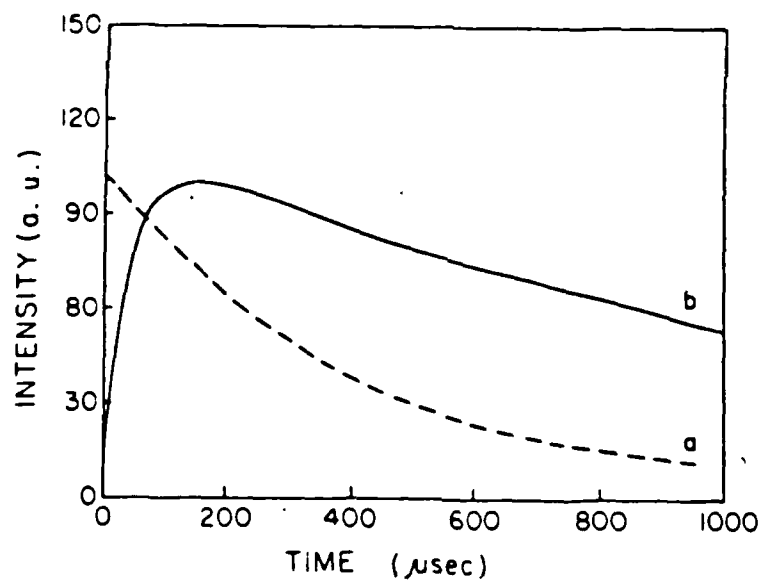


Fig.4 Luminescence decay curves of Nd(III) in ZBLA glass ($55.75\text{ZrF}_4, 33.75\text{BaF}_2, 4.5\text{LaF}_3, 4\text{AlF}_3, 1\text{MnF}_2, 1\text{NdF}_3$). a) Direct excitation of Nd(III) at 579 nm. Lifetime 340 μsec . b) Excitation of Mn(II) at 404nm. Lifetime 1450 μsec .

Quantitative calculation of energy transfer between Mn(II) and Nd(III) in PBLA glass was performed by the steady state and dynamic measurements. The

results of the calculations using the two methods [43] are presented in Table VIII.

Table VIII. Efficiency of energy transfer from Mn(II) to Nd(III) in PBLA glass ($35\text{PbF}_2, 24\text{MnF}_2, 35\text{GaF}_3, \text{AlF}_3, (4-x)\text{LaF}_3, x\text{NdF}_3$)

X	EXCITATION WAVELENGTH	EFFICIENCY FROM:		TRANSFER RATE[sec ⁻¹]
		DECAY TIME	STEADY STATE	
0.2	407	0.52	0.57	1040
0.2	337	0.57	0.56	1550
2.0	407	0.94	0.93	14400
2.0	337	0.92	0.92	12700

A fair agreement between the two series of results using steady state and dynamic measurements indicates that the two methods are mutually consistent in respect to the system studied.

The transfer rates indicate that the transfer proceeds according to a first-order kinetics, the concentration of Mn(II) being constant and concentration of Nd(III) variable. The transfer rates depend strongly on the concentration of Mn(II); the transfer rate for higher concentration of Mn(II) is larger as the Mn-Nd distance decreases. The conclusion being in full accord with intuition nevertheless raises the question whether the kinetics depend on the concentration of ground state Mn(II) ions or rather on the concentration of the excited ions. In our work we observed a systematic trend of faster transfer rates and shorter lifetimes of Mn(II) in presence of Nd(III) when the samples were excited at 337nm. The intensity of the 337nm light from the nitrogen laser is, in our case, a factor of 10 higher than the 407nm light from a dye laser, and the oscillator strength of Mn(II) at 337nm is some 5 times lower than at 407nm. Thus we can expect a twofold increase in excited Mn(II) concentration in the case of excitation at 337nm. If the transfer rates were dependent on the concentration of the excited Mn(II) ions we would then expect an increase in transfer rate, decrease in the lifetime of Mn(II), decrease in the risetime of luminescence of Nd(III) $^4\text{F}_{3/2}$ level and decrease in the lifetime of the same level. The experimental results favor the excited state concentration dependence.

7. SUMMARY

Energy transfer between manganese and neodymium ions in the system studied proceeds through at least three distinct channels;

1- Radiative energy transfer from neodymium to manganese ions in the range of 27700 cm^{-1} to 22000 cm^{-1} .

2- Nonradiative energy transfer from manganese to neodymium ions. The energy transfer occurs probably among the lowest manifold of manganese and a number of levels of neodymium in the range of 25000 cm^{-1} to 20000 cm^{-1} .

The transfer rate of the process is almost linear with concentration of neodymium ions, from 0.2 mole% of neodymium to 2.0 mole% at constant 24 mole% of manganese. At low concentration of neodymium the manganese serves as an efficient storage of energy, which results in the lifetime of neodymium with a factor 2-3 longer than its intrinsic lifetime. The phenomena may be utilized in a Q-switched Nd laser for energy storage

3- Radiative energy transfer from manganese to neodymium ions. The radiation emitted by manganese is absorbed by the $G_{5/2}$ band of Nd(III) in the region around 600 nm.

There is evidence pointing towards the role which the intensity of the exciting light plays in respect to the rate of energy transfer between Mn(II) and Nd(III) in the system investigated.

A series of experiments is planned in order to study the dependence of the energy transfer rate on the intensity of exciting light, as well as a number of computer simulations of the appropriate model.

The systems studied are particularly suitable for a theoretical analysis; the PBLA samples represent an almost ideal case of acceptors Nd(III) which do not interact strongly one with another ($36\text{PbF}_2, 24\text{MnF}_2, 35\text{GaF}_3, 2\text{AlF}_3, 3.8\text{LaF}_3, 0.2\text{NdF}_3$) and a similar case but with a moderately strong interaction among the acceptors ($36\text{PbF}_2, 24\text{MnF}_2, 35\text{GaF}_3, 2\text{AlF}_3, 2\text{LaF}_3, 2\text{NdF}_3$).

On the other hand the $55.75\text{ZrF}_4, 33.75\text{BaF}_2, 4.3\text{LaF}_3, 4\text{AlF}_3, 1\text{MnF}_2, 1\text{NdF}_3$ glass represents a system in which there is a moderate interaction between the donors and weak interaction between the acceptors at equal concentrations of both. Finally by examining Table VII we come to the conclusion that Nd(III) in fluoride glasses has good laser qualities and could be incorporated into fiber optics systems as an integrated light source.

ACKNOWLEDGEMENT: Research partly supported by US Air Force Weapon Laboratory AFB New Mexico, under Contract No. F29601-81-C-0012.

The author is very grateful to Prof C.K. Jørgensen and Dr. M. Eyal for discussion and to Mrs. Esther Greenberg for her help in preparing this work.

REFERENCES

1. Poulain, M., Poulain, M. and Lucas, J., Mater. Res. Bull. 10, 243 (1975).
2. Poulain, M., Chanthanasinh, M. and Lucas, J., Mater. Res. Bull. 12, 151 (1977).
3. Poulain, M. and Lucas, J., Verres Refract. 32, 505 (1978).
4. Tran, D. C., Sigel, Jr. G. H. and Bendow, B., J. Lightwave Technology, LT-2, 566 (1984).
5. Miranday, J. P., Jacoboni, C. and De Pape, R., J. Noncryst. Solids 43, 393 (1981).
6. Miranday, J. P., Jacoboni, C. and De Pape, R., Rev. Chim. Miner. 16, 277 (1979).
7. Reisfeld, R., Greenberg, E., Jacoboni, C., De Pape, R. and Jørgensen, C. K., J. Solid State Chem. 53, 236 (1984).
8. Eyal, M., Greenberg, E., Reisfeld, R. and Spector, N., Chem. Phys. Lett. 117, 108 (1985).
9. Adam, J. L. and Sibley, W. A., J. Noncryst. Solids 76, 267 (1985).
10. Reisfeld, R., Greenberg, E., Brown, R. N., Drexhage, M. G. and Jørgensen, C. K., Chem. Phys. Lett. 95, 91 (1983).
11. Tanimura, K., Shinn, M. D., Sibley, W. A., Drexhage, M. G. and Brown, R. N., Phys. Rev. B 30, 2429 (1984).
12. Reisfeld, R., Eyal, M., Greenberg, E. and Jørgensen, C. K., Chem. Phys. Lett. 118, 25 (1985).
13. Reisfeld, R., Katz, G., Jacoboni, C., De Pape, R., Drexhage, M. G., Brown, R. N. and Jørgensen, C. K., J. Solid State Chem. 48, 323 (1983).
14. Reisfeld, R., Katz, G., Spector, N., Jørgensen, C. K., Jacoboni, C. and De Pape, R., J. Solid State Chem. 41, 253 (1982).
15. Shinn, M. D., Sibley, W. A., Drexhage, M. G. and Brown, R. N., Phys.

- Rev. B. 27, 6635 (1983).
16. Lucas, J., Chanthanasinh, M., Poulain, M., Poulain, M., Brun, P. and Weber, M. J., J. Noncryst. Solids 27, 273, (1978).
 17. Ohishi, Y., Mitachi, S., Kanamori, K. and Manabe, T., Phys. Chem. Glasses 24, 135 (1983).
 18. Reisfeld, R., Proc. Int'l. Symp. on Rare Earth Spectroscopy, Wroclaw, Poland, 1984. World Scientific Pub. Co. PTE. Ltd. 587 (1985).
 19. Reisfeld, R., Eyal, M., Jørgensen, C.K., Guenther, A.H. and Bendow, B., Chimia (in publication).
 20. Bendow, B., Banerjee, P. K., Lucas, J., Fonteneau, G. and Drexhage, M. G., J. Am. Ceramic Soc., 68, C92 (1985).
 21. Jørgensen, C. K., Oxidation Numbers and Oxidation States, Springer-Verlag, Berlin (1969).
 22. Jørgensen, C. K., Modern Aspects of Ligand Field Theory, North-Holland, Amsterdam (1971).
 23. Jørgensen, C. K., Pappalardo, R. and Rittershaus, E., Z. Naturforsch. 20a, 54 (1965).
 24. Reisfeld, R., Rep. Ser. Swedish Acad. Engineering Sciences in Finland (Proc. Advanced Summer School on Electronic Structure of New Materials, Loviisa, Finland, 1984) 40, part I, 7 (1985).
 25. Ferguson, J., Guggenheim, H. J. and Wood, D. L., J. Chem. Phys. 54, 504 (1971).
 26. Andrews, L. J., Lempicki, A. and McCollum, B. C., J. Chem. Phys. 74, 5526 (1981).
 27. Reisfeld, R. and Kisilev, A., Chem. Phys. Lett. 115, 457 (1985).
 28. Reisfeld, R., Kisilev, A., Greenberg, E., Buch, A. and Ish-Shalom, M., Chem. Phys. Lett. 104, 153 (1984).
 29. Kisilev, A., Reisfeld, R., Greenberg, E., Buch, A. and Ish-Shalom, M., Chem. Phys. Lett. 105, 405 (1984).
 30. Bouderbala, M., Boulon, G., Reisfeld, R., Buch, A., Ish-Shalom, M. and Lejus, A. M., Chem. Phys. Lett. 121, 535 (1985).
 31. Rudorff, W., Kandler, J. and Babel, D., Z. anorg. Chem. 317, 261 (1962).
 32. Smith, D. W., J. Chem. Phys. 50, 2784 (1969).
 33. Cramer, S. P. and Hodgson, K. O., Inorg. Chem. 25, 1 (1979).
 34. Reisfeld, R. and Jørgensen, C. K., Lasers and Excited States of Rare Earths, Springer-Verlag, Berlin (1977).
 35. Nielson, C. W. and Koster, G. F., Spectroscopic Coefficients for the p^n , d^n and f^n Configurations (MIT Press, Cambridge, 1964).
 36. Weber, M. J., Proc. Int'l. Conf. on Lasers '82, New Orleans, Dec. 13-17 (1982).
 37. Reisfeld, R. and Eyal, M., J. de Physique, Colloque 7, 349 (1985).
 38. Stokowski, S. E. and Weber, M. J., Laser Glass Handbook M-95, Lawrence Livermore National Laboratory, California 1979.
 39. Reisfeld, R., Kisilev, A. and Jørgensen, C. K., Chem. Phys. Lett. 111, 19 (1984).
 40. Kisilev, A. and Reisfeld, R., Solar Energy 33, 163 (1985).
 41. Bornstein, A. and Reisfeld, R., J. Noncryst. Solids 50, 23 (1982).
 42. Blanzat, B., Boehm, L., Jørgensen, C. K., Reisfeld, R. and Spector, N., J. Solid State Chem. 32, 185, (1980).
 43. Reisfeld, R., Eyal, M., Jørgensen, C. K., Jacoboni, C. and De Pape, R., Chem. Phys. Lett. (1986) submitted.

END
DATE
FILMED
5-88
DTIC